Journal of Catalysis **181,** 175–188 (1999)
Article ID jcat.1998.2310, available online at http://www.idealibrary.com on IDEAL®

Bifunctional Catalysis of Mo/HZSM-5 in the Dehydroaromatization of Methane to Benzene and Naphthalene XAFS/TG/DTA/MASS/FTIR Characterization and Supporting Effects

Shetian Liu,[1] Linsheng Wang,[2] Ryuichiro Ohnishi, and Masaru Ichikawa[3]

Catalysis Research Center, Hakkaido University, Kita-Ku, N-11, W-10, Sapporo 060, Japan

Received March 30, 1998; revised September 12, 1998; accepted October 19, 1998

The direct conversion of methane to aromatics such as benzene and naphthalene has been studied on a series of Mo-supported catalysts using HZSM-5, FSM-16, mordenite, USY, SiO_2, and Al_2O_3 as the supporting materials. Among all the supports used, the HZSM-5-supported Mo catalysts exhibit the highest yield of aromatic products, achieving over 70% total selectivity of the hydrocarbons on a carbon basis at 5–12% methane conversion at 973 K and 1 atm. By contrast, less than 20% of the converted methane is transformed to hydrocarbon products on the other Mo-supported catalysts, which are drastically deactivated, owing to serious coke formation. The XANES/EXAFS and TG/DTA/mass studies reveal that the zeolite-supported Mo oxide is endothermally converted with methane around 955 K to molybdenum carbide (Mo_2C) cluster (Mo-C, C.N. = 1, $R = 2.09$ Å; Mo-Mo, C.N. = 2.3–3.5; $R = 2.98$ Å), which initiates the methane aromatization yielding benzene and naphthalene at 873–1023 K. Although both Mo_2C and HZSM-5 support alone have a very low activity for the reaction, physically mixed hybrid catalysts consisting of 3 wt% Mo/SiO_2 + HZSM-5 and Mo_2C + HZSM-5 exhibited a remarkable promotion to enhance the yields of benzene and naphthalene over 100–300 times more than either component alone. On the other hand, it was demonstrated by the IR measurement in pyridine adsorption that the Mo/HZSM-5 catalysts having the optimum SiO_2/Al_2O_3 ratios, around 40, show maximum Brönsted acidity among the catalysts with SiO_2/Al_2O_3 ratios of 20–1900. There is a close correlation between the activity of benzene formation in methane aromatization and the Brönsted acidity of Mo/HZSM-5, but not Lewis acidity. It was found that maximum benzene formation was obtained on the Mo/HZSM-5 having SiO_2/Al_2O_3 ratios of 20–49, but substantially poor activities on those with SiO_2/Al_2O_3 ratios smaller and higher than 40. The results suggest that methane is dissociated on the molybdenum carbide cluster supported on HZSM-5 having optimum Brönsted acidity to form CH_x ($x > 1$) and C_2-species as the primary intermediates which are oligomerized subsequently to aromatics such as benzene and naphthalene at the interface of Mo_2C and HZSM-5 zeolite having the optimum Brönsted acidity. The bifunctional catalysis of Mo/HZSM for methane conversion towards aromatics is discussed by analogy with the promotion mechanism on the Pt/Al_2O_3 catalyst for the dehydro-aromatization of alkanes. © 1999 Academic Press

Key Words: **bifunctional role; methane conversion; benzene; Mo/ZSM-5; methane aromatization; Mo/HZSM-5 catalysts; XAFS/TG/DTA/IR characterization.**

1. INTRODUCTION

The catalytic conversion of methane to petrochemical feed stocks such as ethylene and benzene has been of current importance and industrial interest in the effective utilization of carbon resources of natural gas. Several one-step catalytic processes converting methane to valuable products have been studied during the past 20 years, including the oxidative coupling of methane (OCM) to ethene (or ethane), selective oxidation of methane to methanol/formaldehyde, and the homologation of methane to lower hydrocarbons (1–6). Nevertheless the industrial interests in these processes have been limited so far because of low product selectivity at higher conversion of methane. During the past five years, the nonoxidative conversion of methane to benzene has been reported by Wang, Xu, and Guo (7, 8), Solymosi (9–12) , and Lunsford (16, 17) on HZSM-5 zeolite-supported Mo catalysts in conjunction with their reactivities, reaction mechanism, and catalyst characterization by XPS (10, 12), XRD, and NMR (13, 14). Moreover, there have been subsequent works by Solymosi (9–12) and Lunsford (16, 17) on the role of the acidity sites of HZSM-5 and the carburization mechanism of Mo oxide on HZSM-5 with methane to form Mo carbide which is proposed to be an active species for the dehydrocondensation of methane towards benzene on Mo/HZSM catalysts. Recent works by Lunsford (17) and Ichikawa (18, 19) demonstrated that methane is actually dehydrocondensed into various aromatics, not only benzene, but also naphthalene on Mo/HZSM-5 and the Fe/Co promoted Mo/HZSM-5 at 873 K–973 K. Since the pioneering works by Wang, Liu, and Xu in 1993 (7), a number of previous papers have

[1] On leave from Hebei University of Science and Technology, Shijiazhuang 050018, China.
[2] On leave from Dalian Institute of Chemical Physics, Dalian, China.
[3] Corresponding author. E-mail: michi@cat.hokudai.ac.jp.

0021-9517/99 $30.00

been concerned only about the methane conversion to benzene on Mo/HZSM-5. Regarding the quantitative study on methane aromatization, the authors are concerned how to reasonably evaluate the product yields and the coke formation in this process, and they found, using the improved analytic system of on-line GC/MS and the high-molecular TOF-mass analyzer, that coke formation in the methane aromatization reaction is much more serious than had been expected and the benzene formation is not so selective on Mo/HZSM-5. Actually, there are a number of various aromatic compounds and undetected hydrocarbons formed during the reaction.

In this report, we study carefully the activities and selectivities of methane conversion to aromatics and coke formation on the Mo-supported catalysts by varying the supporting materials. The Mo/HZSM-5 catalysts are characterized by EXAFS, TG/DTA/mass, and TPR (temprature-programmed reaction) studies, including the carburization of Mo oxide with methane towards Mo_2C. The acidity measurement of Mo/HZSM-5 having different Si/Al ratios has been conducted by IR spectroscopy in the pyridine adsoprtion. The bifunctional role of molybdenum carbide and HZSM-5 zeolite is discussed in conjunction with the active states of Mo and the Brönsted and Lewis acidity function of HZSM-5 supports having different Si/Al ratios which affect the activity and selectivity of methane conversion towards benzene and naphthalene, as well as coke selectivity in the reaction.

2. EXPERIMENTAL

2.1. Materials and Catalysts Preparation

The Mo-supported catalysts were prepared using either an incipient wetness or a conventional impregnation method. The materials used are: $(NH_4)_6Mo_7O_{24}\cdot 4H_2O$ (Kanto Chem. Co.); NH_4ZSM-5 ($SiO_2/Al_2O_3 = 20 \sim 1900$; surface area, 780–925 m^2/g (Toso Co. and CRI Zeolyst, Inc., as purchased); Al_2O_3 (Japan Aerosil Co., 280 m^2/g), SiO_2 (Japan Aerosil Co., 350 m^2/g), FSM-16 (gift from Toyota Central Research Lab.; pore sizes = 4.7 nm and 2.7 nm; $SiO_2/Al_2O_3 = 320$; 980–1020 m^2/g), and H-Mordenite ($SiO_2/Al_2O_3 = 44$; Cat. & Chem. Ind.. Co. Ltd.). The modified FSM-16 having Si/Al ratios of 15 and 20 were prepared by CVD technique with $AlCl_3$. The Al-contents in the HZSM-5, H-mordenite, and FSM-16 supports were analyzed by ICP measurements of the samples dissolved with HF solution. The 3–6 wt% Mo loading HZSM-5 catalysts were prepared by impregnation of NH_4ZSM-5 with $(NH_4)_6Mo_7O_{24}\cdot 4H_2O$ (Kanto Co., as purchased) from an aqueous solution and an incipient wetness technique. The resulting materials are dried at 393 K and calcined at 773 K for 6 h, similarly as reported in the literature (18). Powdered Mo carbide (Mo_2C; 1.8-μm size, surface area of 1–2 m^2/g) was purchased from Japan New Metal Co. and used as it.

The hybrid catalysts of 3 wt% Mo/SiO_2 + HZSM-5 were prepared by mechanically mixing and grinding both components in pyrex-glass tubing and Mo_2C + HZSM-5 was prepared by the coimpregnation of both component powders from the slurry solution, which were pressed in a pellet, crushed into sizes of 20–42 mesh for catalytic tests.

2.2. Catalytic Measurements and Product Analysis

The catalytic tests were carried out under atmospheric pressure of methane in a continuous flow system with a quartz reactor of 8-mm ID which is charged with 0.30 g of catalyst pelleted and sized to 20–42 mesh. The outlet pipe line from the reactor and the on-line sampling valve were kept at higher than 500 K to prevent the condensation or strong adsorption of the higher hydrocarbon products, as shown in Fig. 1. The feed gas mixture of 98% CH_4 (99.9% purity) and 2% Ar (Daido Hoxan Inc., 99.9% purity) as the internal standard for analysis was introduced into the reactor at 7.2 mL/min, controlled with a mass flow controller (Brooks Co.) after flushing with He at 973 K for 40 min. The Shimadzu GC-14A gas chromatograph with a flame ionization detector (FID) is equipped with a six-way valve heating at 260°C for sampling and separation of hydrocarbon products including nonvolatile compounds, such as benzene derivatives and naphthalene on a 4 mm × 1 m Porapak-P column. Another GC of Shimadzu GC-8A was employed for on-line product analysis of H_2, Ar, CO, CH_4, and CO_2 on a 4 mm × 2 m activated-carbon column with a thermal conductivity detector (TCD). Hydrocarbons produced in this reaction were C_2-C_4 alkanes (and/or alkenes) and C_6-C_{12} condensable materials such as such as benzene, toluene, xylene, naphthalene, and methyl-naphthalene which were identified by using on-line GC and GC-MS (Perkin-Elmer, Auto System GC with 910 Q-Mass) spectrometer.

The total gas flow rate at the inlet and outlet of the reactor can be described as shown in Eq. [1] since the mass flow rate of Ar as an internal standard gas should be constant through the reaction progress. By use of Eq. [1], conversion of methane (Conv.) and selectivity of each product containing a carbon atom, including CO and CO_2 on carbon base ($S^{\text{carbon}}_{\text{product}}$) is calculated from Eqs. [2] and [3], respectively. Thus, the selectivity for coke formation on a carbon basis is derived from (1 − the sum of product selectivity). Coke consists of all undetected carbon products such as amorphous and graphic inert carbons, including higher boiling compounds which are difficult to detect and analyze by the FID and TCD gc used. In these equations, F, X, and N_{carbon} represent the total gas flow rate, mole fraction, and carbon number in a molecule, respectively. Similarly, selectivity for the formation of a hydrogen-containing product on a hydrogen base can be calculated and, thus, the ratio of hydrogen to carbon in the coke formed can be

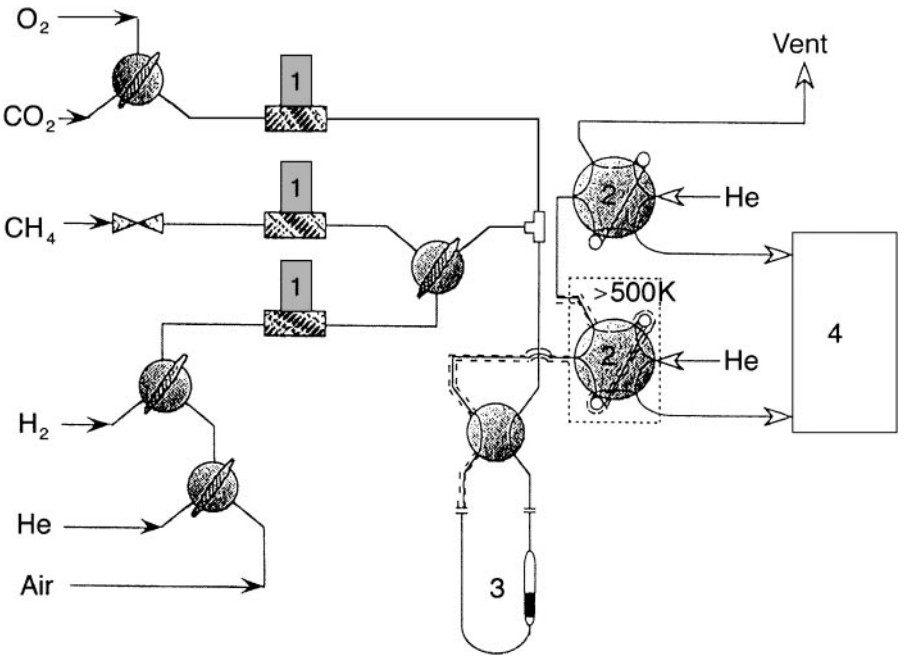

FIG. 1. Schematic flow system: (1) mass flow controller (MFC); (2) heating 6-way valve; (3) quartz cell containing a catalyst; (4) gas chromatograph (FID, TCD).

estimated:

$$F^{\text{inlet}} \times X^{\text{inlet}}_{\text{Ar}} = F^{\text{outlet}} \times X^{\text{outlet}}_{\text{Ar}}. \quad [1]$$

The rate of methane consumption is expressed by $F^{\text{inlet}} \times X^{\text{inlet}}_{\text{CH}_4} - F^{\text{outlet}} \times X^{\text{outlet}}_{\text{CH}_4}$. Thus, methane conversion is estimated:

$$\text{Conv.} = \frac{F^{\text{inlet}} \times X^{\text{inlet}}_{\text{methane}} - F^{\text{outlet}} \times X^{\text{outlet}}_{\text{methane}}}{F^{\text{inlet}} \times X^{\text{inlet}}_{\text{methane}}} = 1 - \frac{X^{\text{outlet}}_{\text{methane}} \times X^{\text{inlet}}_{\text{Ar}}}{X^{\text{inlet}}_{\text{methane}} \times X^{\text{outlet}}_{\text{Ar}}} \quad [2]$$

$$S^{\text{carbon}}_{\text{product}} = \frac{F^{\text{outlet}} \times X^{\text{outlet}}_{\text{product}} \times N^{\text{carbon}}_{\text{product}}}{F^{\text{inlet}} \times X^{\text{inlet}}_{\text{methane}} - F^{\text{outlet}} \times X^{\text{outlet}}_{\text{methane}}} = \frac{X^{\text{inlet}}_{\text{Ar}} \times X^{\text{outlet}}_{\text{product}} \times N^{\text{carbon}}_{\text{product}}}{X^{\text{outlet}}_{\text{Ar}} \times X^{\text{inlet}}_{\text{methane}} - X^{\text{inlet}}_{\text{Ar}} \times X^{\text{outlet}}_{\text{methane}}}. \quad [3]$$

2.3. TG/DTA/Mass Experiment for Carburization of Mo/HZSM-5

TG/DTA/Mass study was performed using TG/DTA/MASS System (Mac Science Co., TG-DTA2020S) under a methane/He stream (flow rate: $CH_4 = 15$ ml/min and $He = 150$ ml/min) and H_2/He (170 ml/min); 40–100 mg of Mo/HZSM-5 catalyst were mounted in a fused alumina boat and the products developed, such as H_2, CO, CO_2, C_2H_4, C_2H_6, C_6H_6, and $C_{10}H_8$ were continuously monitored with a TE-150 multiple channel mass spectrometer (ThermoLab, VG Gas) at m/e = 2, 28, 44, 26, 30, 78, and 128, respectively. The reaction temperature was raised from room temperature to 973 K with a ramping rate of 10 K/min and held there for 30 min. Before the reaction started, the catalyst was heated in a He stream at 873 K for 30 min and, in some cases, was further pretreated with H_2, methane, or ethane at 873 or 973 K for 30 min.

2.4. XAFS Measurement and Analysis

The powdered and disk samples were charged under N_2 in an *in-situ* XAFS cell with a Kapton film window (500 μm) to prevent exposure of the sample to air. Mo K-edge XAFS (X-ray absorption fine structure) measurements were conducted on the samples of Mo/HZSM-5 after impregnation, calcination at 873 K, and reaction with methane at 873 K and 973 K at BL-10B at the Photon Factory of the National Laboratory for High Energy Physics (KEK-PF, Tsukuba, Japan). The energy and the current of the electron (or positron) were 2.5 GeV and 250 mA, respectively. A Si(311) channel-cut monochromator was used. The XANES (X-ray absorption near edge structure) and EXAFS (extended X-ray absorption fine structure) spectra were analyzed by a computer program supplied by Technos Co. LTD [20]. The k^3-weighted EXAFS function was Fourier transformed into R-space using the k-range from 3.5 to 18 Å^{-1}. The Hanning function used was $\delta = 0.5$ Å^{-1}. The phase shift was not corrected for the preliminary Fourier transformation.

The inverse Fourier transform was calculated to obtain a filtered EXAFS function. The R range of an inverse Fourier transformation was taken from 1.09 to 3.31 Å. The Hanning function of $\Delta = 0.05$ Å was used as a window function. The fitting EXAFS parameters of the sample were determined for coordination number (C.N.) and interatomic distance R, to minimize σ and correction of threshold energy (ΔE_o). The backscattering amplitudes and phase shift functions of Mo-Mo, Mo-C, and Mo-O bondngs are corrected using those of Mo foil (Mo-Mo), Mo_2C (Mo-Mo, Mo-C), and MoO_3 (Mo-Mo, Mo-O). The EXAFS parameters for discussion were fixed around the optimum value, and the residual factor R was calculated to offer the optimum values for the other parameters. The real value was estimated using a residual factor R which is smaller than twice the optimum value.

2.5. IR Measurement in Pyridine Adsorption

Each powder of 3 wt% loading Mo/HZSM-5, having a different silica to alumina ratio, $SiO_2/Al_2O_3 = 20$–1900, was pressed into a self-supporting wafer (2.0 mm ID, 15–18 mg/cm^2) with a pressure of 500 kgf/cm^2. The wafer was mounted in an *in-situ* IR cell equipped with CaF_2 window. IR spectra were recorded using a step-scan Fourier transform infrared spectrometer (BIO-RAD FTS-60A/896) with resolution of 4 cm^{-1}, and a co-accumulation of 64 interferograms to improve the signal/noise ratios of the IR spectra. The IR measuremnt was conducted by exposure of the disk of HZSM-5 after evacuating at 723 K for 2 h to the pyridyne vapor of 1.2 kPa at 300 K.

3. RESULT AND DISCUSSION

3.1. The Reaction of Methane on 3% Mo/HZSM-5 and Product Analysis

The catalytic performance of 3% Mo/HZSM-5 for methane aromatization at 973 K and 1 atm pressure of methane has been described in our previous study (18). Hydrogen is usually produced in large amounts (H_2/benzene = 9–18 mol/mol) by the dehydrocondensation of methane. CO, CO_2, and H_2O are evolved at the initial stage of the reaction above 873 K, due to the reduction of MoO_3 with methane, being converted to a lower valent state species or molybdenum carbide (9, 16–18). Methane conversion and the product formation rates with reaction time on-stream are illustrated in Fig. 2a. The conversion of methane (ca 12%) usually decreases rapidly at the initial stage and moderately at the later stage of the reaction, down to 4% in 30 h of the time on-stream. The suppression of methane conversion may be attributable to coke formation upon the admission of methane to the fresh Mo/HZSM-5. This suggests that the deposited carbon becomes less reactive with time on-stream, which also leads to the gradual deactivation of the catalyst. The major hydrocarbons produced on Mo/HZSM-5 consist of benzene, naphthalene, and toluene as the aromatics and C_2 products such as ethene and ethane. The other carbon-containing products, such as CO, propene, butene, methyl-naphthalene, phenanthrene, and anthracene were only produced in trace amounts (totaling a few percentages of selectivity). Figure 2b shows the selectivity of hydrocarbon products such as benzene, naphthalene, and C_2 species and the coke formation with time on-stream of methane at 973 K. The total selectivity of gas phase hydrocarbon products increases from 55% at the initial stage of the reaction and then keeps constant (70%) at the steady state of the reaction, while the selectivity of coke formation changes in a reverse way from 43 to 32%. The selectivity of CO is less than 1% throughout the reaction. This may suggest that hydrocarbon products and coke share a common intermediate such as CH_x leading in part to C_2 species and hydrocarbon products and in part to coke formation.

Figure 2c shows the compositions in the gas phase hydrocarbon products on 3% Mo/HZSM-5 catalyst with the time on stream of the methane reaction. At the initial stage of the reaction C_2 species, benzene, toluene, and naphthalene are produced in 4%, 50%, 2%, and 45% on a carbon basis, among the produced hydrocarbons, respectively. After running the reaction 24 h the percentage of naphthalene among the hydrocarbon products decreases from 45% to 12%, while the percentage of C_2 and benzene increase to about 20% and 68% at the expense of the decrease of naphthalene. This may suggest that naphthalene is apparently produced consecutively from C_2 species and benzene. As shown in Fig. 2d, the rates of benzene and naphthalene formation in the methane aromatization reaction decreased monotonously from the maximum rates of 98 to 50 nmmol/s · g-cat after 30 h, possibly by catalyst poisoning due to the irreversible coke deposition. The molar ratios for toluene to benzene and methylnaphthalene to naphthalene are almost held constant at 3–5% during the entire reaction process. Further substituted aromatic compounds are obtained in negligible amounts on the Mo/HZSM-5, partly because of the higher activity of hydrogenolysis and molecular shape selectivity due to the limited size of micropores of HZSM-5 that are accessible only to benzene and toluene.

Using 2% Ar as the internal standard for the reaction analysis, the present work has been conducted to carefully evaluate the yields and selectivities of benzene formation in the reaction. The results we obtained show that the benzene selectivities, based on the methane consumed, did not exceed 48% as the maximum value and that of coke formation is 32–43%, which differs greatly from the estimates of Wang *et al.* (16, 17) and others (7, 9, 13, 15). This large discrepancy may be mainly due to the analytic accuracy of the methane concentration consumed using the internal standard of Ar (18) and N_2 (16, 17) in a different concentration and

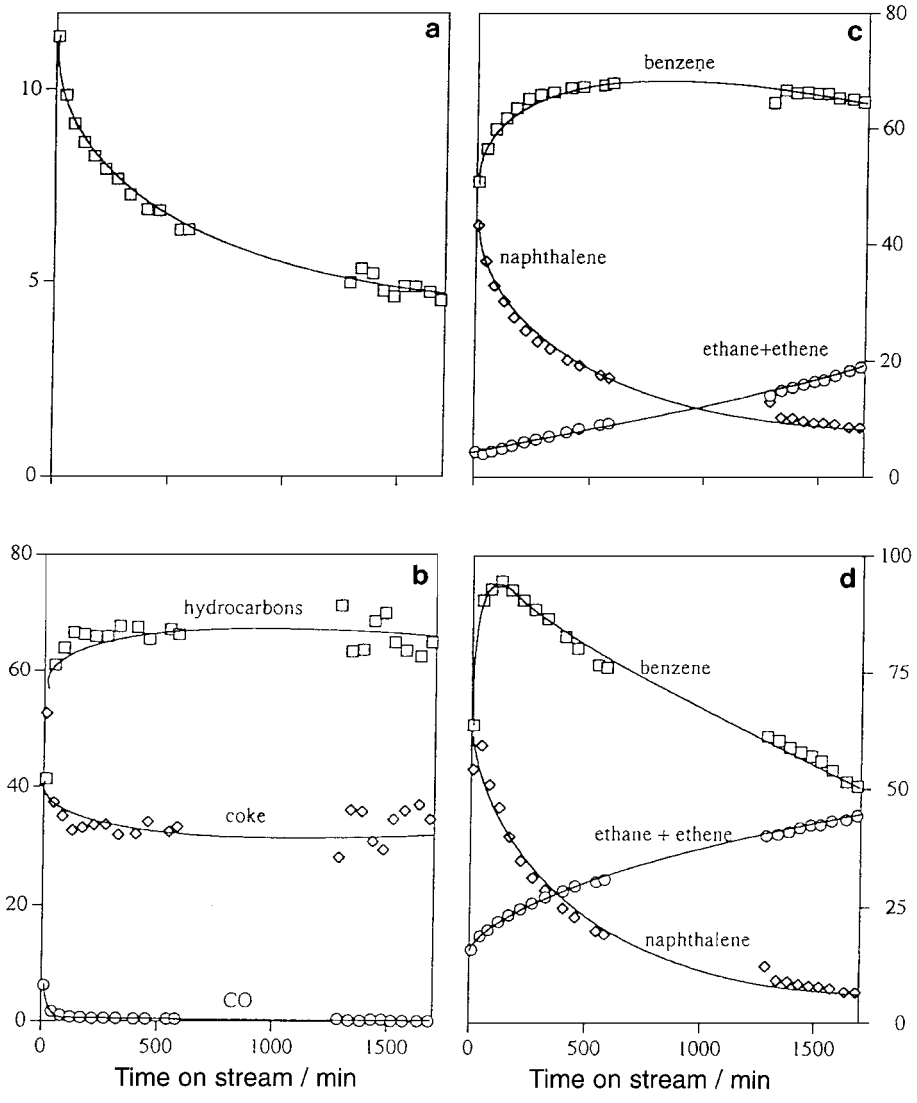

FIG. 2. Catalytic performances in methane aromatization on 3 wt% Mo/HZSM-5 at 973 K: (a) methane conversion vs time on-stream; (b) selectivities (%) on carbon base for hydrocarbon products, coke, and CO vs time on-stream; (c) composition (%) in hydrocarbon products; and (d) rates of product formation for benzene, naphthalene, and C_2 species (nmol/s · g-cat).

neglecting the higher polycondensed hydrocarbons such as naphthalene, methylnaphthalene, and anthracene as the products in the reaction (7–16). To confirm this, we have analyzed all of the products in the effluent gas which are condensed by using the ethanol–dry ice trap. The collected reaction products were analyzed by the on-line GS/Mass with a capillary column (OV-1; 25 m) up to 553 K and MALDI-TOF (time-of flight reflect-mass spectrometer; VOYAGER; m/e = 1–2500; PerSeptive Biosystems Co.) mass sepctromtery. Table 1 shows a list of aromatic compounds, such as benzene and naphtalene as the major products, including other polycondensed aromatics such as anthracene, pyrene, tetracene, and their deriviates which were collected as products of the methane reaction on 3 wt% Mo/HZSM-5 at 973 K. The latter part of the polycondensed aromatic compounds are difficult to analyze by the on-line GC system due to their high boiling point and strong adsorption on the separation column. The total mount of such polycondensed products is estimated to be not over 10% of the detected hydrocarbons, such as benzene and naphthalene. The most distinct feature is that the conversion of methane usually decreases monotonously with time on-stream, while the total selectivity of all the hydrocarbon products keeps constant.

3.2. Reaction of Methane on 3% Mo/FSM-16

Figure 3 shows the time dependencies of methane conversion (3a), the selectivity of hydrocarbon on a carbon basis (3b), the composition (%) of benzene devided by 2

TABLE 1

Distribution of Aromatic Products Formed in the Methane Conversion on the 3 wt% Loading Mo/HZSM-5 Catalyst at 973 K

Aromatic product	Percentage composition on carbon basis
Benzene	67.6
Toluene	3.5
p-Xylene, *m*-xylene	0.1
C_9 aromatics (e.g., methylene, 1,2,4-trimethylbenzene)	0.2
Naphthalene	24.6
Methylnaphthalene	0.7
Dimethylnaphthalene (2,6-)	0.2
C_{13} aromatics (anthracene, phenanthrene)	0.3
Other polycondensed aromatics Pyrene, Teracene, etc.	Less than 2%

Note. The aromatic products were condensed by the cold-trap in the methane reaction for 5 h. Methane pressure = 1 atm, SV = 1440 ml/h/g-cat.

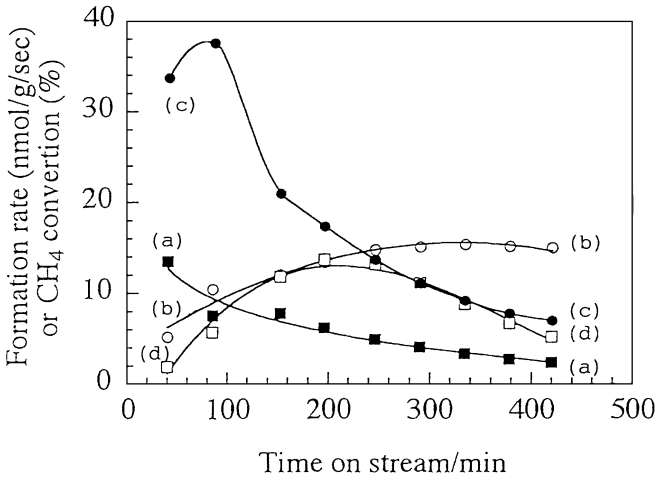

FIG. 3. Catalytic performances in methane aromatization on 3 wt%Mo/FSM-16 (2.8 nm) at 973 K: (a) methane conversion vs time on stream (–■–); (b) selectivity (%) of hydrocarbon products on carbon basis vs time on stream (–○–); (c) composition (%) of benzene devided by 2 in hydrocarbon products (–●–), and (d) rates of product formation for benzene (–□–) (nmol/s/g-cat).

on a carbon basis (3c), and the formation rate of benzene (3d) in the methane reaction at 973 K on 3 wt% Mo loading catalysts prepared by impregnating $(NH_4)_6Mo_7O_{24}$ with the mesoprous material of FSM-16 (2.7 nm; Si/Al = 320). Although benzene and C_2 species with a minor yield of toluene and naphthalene were produced in the methane reaction (1 atm, SV = 1440 ml/h/g-cat) at 973 K, the methane conversion decreases rapidly from 14% at the initial stage to 3% within 6 h, possibly owing to serious coke formation. The formation rate of benzene reaches a maximum value of 10.5 nmol/s/g-cat at 250 min of time on-stream and then decreases while the formation rates of ethene and ethane relatively increase. The steady-state distributions of benzene and C_2 species among the hydrocarbon products (selectivities of the hydrocarbons decreased from 38 to 5% in the time on-stream of the reaction) were 71–74% and 24–27% on a carbon basis, respectively. It is of interest to find that the catalytic performances of Mo-loading catalysts of FSM-16 are not affected with their pore sizes between 2.7 and 4.7 nm, as shown in Table 2. Although the compositions of the hydrocarbon products on the 3% Mo/FSM-16 catalaysts are idential to those on 3% Mo/HZSM-5 as illustrated in

TABLE 2

Catalytic Performances of 3 wt%-loading Mo Catalysts (0.3 g) using Various Supports for CH_4 Aromatization Reaction at 973 K

Catalysts	Conv. (%)	Selectivity (%)			HC distribution (%)[a]			
		HC	Coke	CO	C_2	C_6H_6	C_7H_8	$C_{10}H_8$
3%Mo/HZSM-5 (Si/Al = 79)	9.4	62.8	36.1	1.1	4.5	65.2	3.3	26.9
HZSM-5 (Si/Al = 79)[b]	0.7	12.1	80.8	7.1	82.1	17.9	0.0	0.0
3%Mo/Mordenite	7.3	7.8	83.1	9.1	44.4	53.2	0.0	0.0
3%Mo/USY	6.4	13.2	84.3	2.4	16.9	79.8	3.3	0.0
3%Mo/Al_2O_3	7.4	6.2	88.9	4.9	33.8	63.8	2.4	0.0
3%Mo/SiO_2	5.3	11.5	86.6	1.9	18.6	75.8	3.2	2.4
3%Mo/FSM-16 (2.7 nm)	6.8	9.0	87.7	3.3	24.8	73.4	1.8	0.0
3%Mo/FSM-16 (2.7 nm, Si/Al = 20)	6.6	8.4	89.0	2.5	20.0	77.3	2.8	0.0
3%Mo/FSM-16 (2.7 nm, Si/Al = 15)	5.9	7.8	87.5	4.8	21.9	75.4	2.7	0.0
3%Mo/FSM-16 (4.7 nm)	6.2	11.2	86.1	2.6	24.0	73.6	2.4	0.0

Note. Methane 1 atm, flow rate = 7.6 ml/min.

[a] The data for methane conversion and product selectivity were taken at the initial stage of the reaction in 40 min after the 1 atm methane flow passed through the catalyst bed (less than 3-mm thickness) at 973 K. $C_2 = C_2H_4 + C_2H_6$; C_7H_8 = toluene; $C_{10}H_8$ = naphthalene.

[b] The data were obtained on HZSM-5 support in the methane reaction at 973 K.

Fig. 1 and Table 2, the catalyst deactivation was more dominant than those of the HZSM-5-supported one. In fact, on 3% Mo/FSM-16 having Si/Al ratios of 15–320 the selectivity of coke formation is substantially high (over 80%), in comparison with that of 30–32% on 3% Mo/HZSM-5 for the methane reaction under similar reaction conditions.

3.3. *Effects of the Support of the Catalysts for the Reaction*

The catalytic performances of other 3 wt% loading Mo-supported catalysts using various sorts of supporting materials have been studied in the methane reaction, and the results are listed in Table 2. Comparing with 3% Mo/HZSM-5, although the methane conversions were comparable or relatively lower (5.3–7.4%), the selectivities of the hydrocarbon products (HC), such as C_2-hydrocarbons (C_2) and benzene, on a carbon basis are substantially low due to serious coke formation on the supported catalysts using FSM-16, Mordenite, USY, SiO_2, and Al_2O_3 as the supports. The selectivities of hydrocarbon products in the gas phase were less than 13% (less than 10% for benzene) on a carbon basis, while the coke formation is higher than 80%, as presented in Table 2. The main products for hydrocarbons on these catalysts are ethene, ethane, and benzene. Naphthalene is only produced in a trace amount on these supported catalysts. In the early stage of the reaction, the distribution of C_2 species among the hydrocarbon products range from 20% to 40% which is higher than for those on 3% Mo/HZSM-5 (less than 5%), and for prolonged reaction the C_2 products increase to more than 60%, in spite of the lower methane conversion of less than 1%. The compositions of the hydrocarbon products with reaction times on SiO_2, Mordenite, USY, and Al_2O_3-supported Mo catalysts have a trend similar to those on Mo/FSM-16 having different Si/Al ratios (15, 20, and 320). Regarding the methane conversion on Mo-supported catalysts, the results suggest that the HZSM-5 zeolite having Si/Al = 40 has been so far a better support for the Mo-supported catalysts exhibiting the highest methane conversion and selectivities for the aromatic products with a lower coke formation, probably owing to their acidity and their unique pore structures of 0.6-nm size.

3.4. *Influence of Silica to Alumina Ratios in HZSM-5 on Brönsted Acidity and Methane Aromatization Activity on Mo/HZSM-5*

A series of 3% Mo/HZSM-5 catalysts was prepared using different SiO_2/Al_2O_3 ratios. The performaces in the methane conversion at 973 K have been studied on the catalysts in conjunction with the SiO_2/Al_2O_3 ratio of the support HZSM-5 used as shown in Table 3. Actually, it is of interest to find that the rates of hydrocarbon product formation such as benzene on the Mo/HZSM-5 catalysts substantially depend on the SiO_2/Al_2O_3 ratios of the HZSM-5 used, showing the maximum activities of methane aromatization for the HZSM-5 supports having SiO_2/Al_2O_3 ratio of 30–45. By contast, as shown in Table 3 the Mo/HZSM-5 having smaller and higher SiO_2/Al_2O_3 ratios than the optimum values of 30–45 exhibited poor activities for the benzene formation, smaller by one or two orders of magnitude and more serious coke formation than those on the Mo/HZSM-5 catalyst having a SiO_2/Al_2O_3 ratio of 40. The Brönsted and Lewis acidity of the samples have been determined by pyridine adsorption using FT-IR spectroscopy. Figure 4a shows the IR spectra of pyridine adsorption on 3% Mo/HZSM-5 catalysts with different SiO_2/Al_2O_3 ratios. Upon pyridine adsorption at room temperature and outgassing at 423 K, absorption bands associated with the chemisorbed pyridine were observed at 1547 cm^{-1}, 1491 cm^{-1}, and 1454 cm^{-1}. According to previous reports on the IR studies in the pyridine chemisorption (21, 23), the pyridine band at 1547 cm^{-1} is assignable to pyridinum ions and the band at 1454 cm^{-1} to Lewis acid-coordinated pyridine, respectively. The band at 1491 cm^{-1} consists of bands due to the Brönsted and Lewis sites. All the spectra were normalized using the peak intensities of ZSM-5 support at around 1873 cm^{-1} as the standard, and the intensities of bands at 1547 cm^{-1} for Brönsted acid and 1454 cm^{-1} for Lewis acid sites were used for probing the acidity on the Mo/HZSM-5 catalysts having different SiO_2/Al_2O_3 ratios. It is found as shown in Fig. 4b that there is not an appreciable difference in the IR bands at 1547 cm^{-1} due to the Brönsted acidity on the samples of 3 wt% Mo/HZSM-5 and the HZSM-5 support itself after being calcined at 773 K. This implies that the impregnated Mo species does not change the Brönsted acidity of the HZSM-5 support. By contrast, the band around 1440 cm^{-1}, assignable to the Lewis acid site was relatively increased on the Mo/HZSM-5 after being calcined at 773 K and even after the methane aromatization reaction at 973 K. There is a corelation between the Lewis acidity and the

TABLE 3

Catalytic Performances of 3 wt% Mo/HZSM-5 Catalysts with Different Silica to Alumina Ratio for Methane Aromatization Reaction at 973 K and 1 atm Pressure

		Selectivity (%)		Hydrocarbon products distribution (%)			
Si/Al_2	CH_4 Conv. (%)	HC	Coke	C_2	Benzene	Toluene	Naph.
23.8	8.8	55.2	41.6	4.7	65.4	3.4	26.5
26.0	8.0	54.1	43.6	5.6	67.0	3.7	23.4
39.5	10.2	62.8	35.3	3.9	59.4	3.1	33.2
53.0	7.2	48.1	47.3	7.3	62.9	3.3	26.3
73.4	8.3	35.6	60.9	7.1	66.5	3.5	22.8
216	7.5	16.7	79.3	21.5	59.0	4.0	14.5
800	5.1	30.8	61.4	18.3	64.0	3.6	13.5
1900	6.3	19.7	76.9	26.9	57.0	4.2	10.6

Note. Data are taken at 40 min of reaction time on-stream.

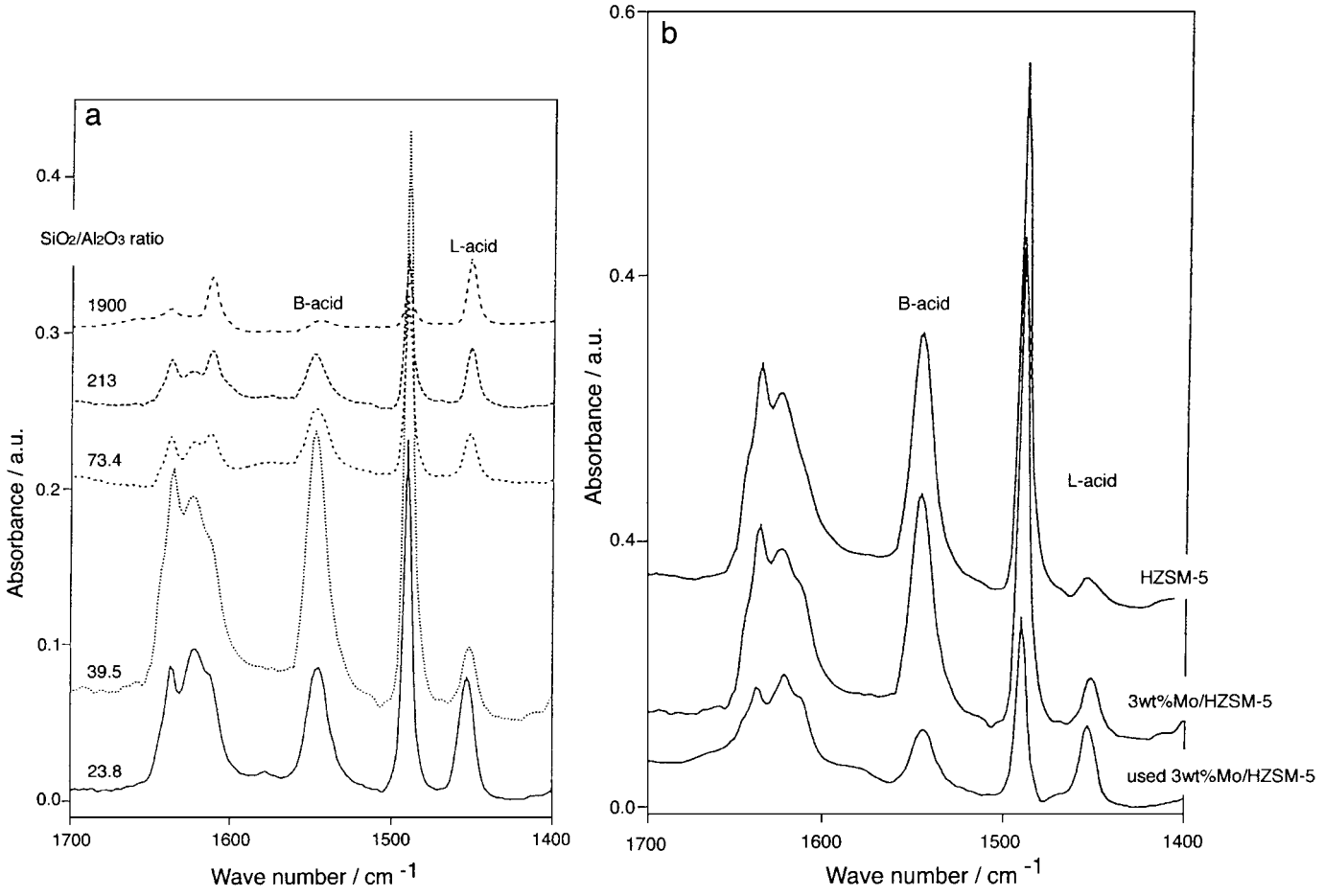

FIG. 4. (a) IR spectra of adsorbed pyridine on 3 wt% Mo/HZSM-5 having various SiO_2/Al_2O_3 ratios; Pyridine of 1.2 kPa was adsorbed at 300 K and evacuated at 423 K for 2 h prior to the IR observation. (b) The change of IR spectra in the pyridine adsorption on the 3 wt% Mo/HZSM-5 (SiO_2/Al_2O_3 ratio of 39.5) before and after the methane reaction at 973 K, compared with that on the HZSM-5 support itself. The samples were calcined at 773 K for 2 h prior to the IR study in pyridine adsorption. The IR spectra were recorded in the pyridine chemisorption after the samples were evaculated at 423 K for 2 h.

lattice-substituted metal ions, such as Al^{3+}, and higher valent Mo species, such as Mo^{6+}.

In Fig. 5, the variations of Brönsted and Lewis acidity on the Mo/HZSM-5 and those of the benzene formation rates and coke selectivities in the methane aromatization on Mo/HZSM-5 catalysts are illustrated against the function of the SiO_2/Al_2O_3 ratios of the HZSM-5 supports used. The Brönsted acidity of HZSM-5 showed a sharp maximum for the HZSM-5 having the SiO_2/Al_2O_3 ratio of 39.5, which is identical to that of benzene formation rates. Nevertheless, there is not a particular relationship between the benzene production and the Lewis acidity of the Mo/HZSM-5 which monotonously decreases with the increase of the SiO_2/Al_2O_3 ratio for the HZSM-5 used.

According to the close correlation between the Brönsted acidity of the Mo/HZSM-5 catalysts and the benzene formation rates in methane aromatization reaction, it is reasonably suggested that the aromatic products such as benzene are most probably promoted by the Brönsted acid sites, not by the Lewis acid ones of the ZSM-5 support. Moreover, as shown in Fig. 5, it was demonstrated that the coke selectivities in the methane conversion on the Mo/HZSM-5 are minimized (less than 30%) for the HZSM-5 having the optimum SiO_2/Al_2O_3 ratio of 39.5, whereas the coke forms seriously up to over 85% on the catalysts using the HZSM-5 with the lower or higher SiO_2/Al_2O_3 ratio deviated from 35–45. Moreover, the acidity measurements of HZSM-5 and 3% Mo/HZSM-5 with SiO_2/Al_2O_3 ratio of 39.5 before and after the methane aromatization reaction also supply us some additional evidence. It is worthy to note that for the 3% Mo/HZSM-5 the intensity of IR band at 1547 cm^{-1} due to the pyridine adsorption on Brönsted acid sites was greatly suppressed after the methane aromatization reaction at 973 K for 8 h, as shown in Fig. 4b. This suppression of Brönsted acidity on the used Mo/HZSM-5 catalyst might be related to the coke deposition in the reaction with methane at 973 K, which plugs the internal channels of HZSM-5, or thermal reaction of methane with acidic

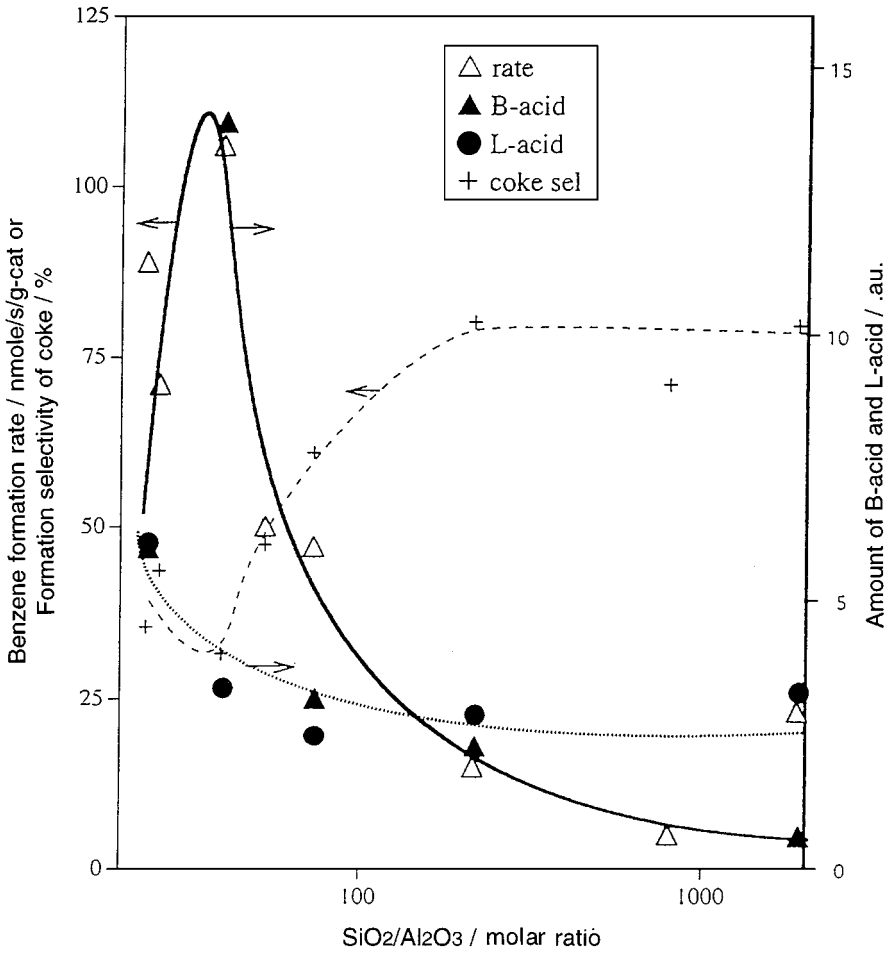

FIG. 5. Dependencies of benzene formation rates (nmol/s/g-cat) and coke selectivitty (%) in the methane reaction at 973 K and those of Brönsted and Lewis acidities deduced by the IR study in pyridine adsorption on the 3 wt% Mo/HZSM-5 upon the SiO_2/Al_2O_3 ratios of the HZSM-5 used.

silanol groups on the Mo/HZSM-5 above 773 K. The latter effect on the Brönsted acidity of HZSM-5 is similar to the preferential decrease of bands at 3611 cm^{-1} due to Brönsted acidic OH of HZSM-5 by heating above 673 K, as recently reported by Lunsford *et al.* (17).

The higher Brönsted acidity of the HZSM-5 supports may bifunctionally promote not only the methane activation ($CH_4 \Rightarrow CH_x + nH_2$) on the Mo carbide sites of Mo/HZSM-5 catalysts, but also a further oligomerization of the dissociative CH_x surface species towards the primary products such as ethene, which are effectively converted into benzene and naphthalene on the Mo/HZSM-5 catalysts.

3.5. Mo Carbide Formation in the Methane Conversion on Mo/HZSM-5 Characterized by TG/DTA/Mass and EXAFS Studies

The X-ray diffraction patterns of calcined or carburized supported samples (Mo/HZSM-5) with up to 6% loading showed no peaks corresponding to molybdenum oxide or molybdenum carbide because of the higher dispersion of both Mo crystallites on the HZSM-5 supports as suggested previously (12, 16, 18). The unsupported Mo_2C sample showed peaks corresponding to Mo_2C of the hexagonal close-packed crystal structure with normal lattice parameters of $a = 2.99$ Å and $c = 4.72$ Å. To characterise the active structure of the Mo/HZSM-5 which is incorporated into the methane aromatization, the Mo K-edge XAFS studies have been conducted using the 10B line at Photon Factory of National Laboratory for High Energy Physics (KEK-PF; Tsukuba, Japan). Figure 6 represents some XANES spectra of 6 wt% loading Mo/HZSM-5 calcined, treated at increasing temperatures in flowing methane at 973 K for 1 and 24 h. The spectra of a MoO_3, Mo foil, and a Mo_2C powder were observed as references. All the spectra (Figs. 6c and 6d) of Mo/HZSM-5 after the carburization with methane at 973 K showed identical edge position, similar to Mo carbide (Fig. 6e) and Mo foil (Fig. 6f) as the first inflection point in the rapidly rising portion of the edge. This position was assigned an energy of 20003.9 eV. It is known that

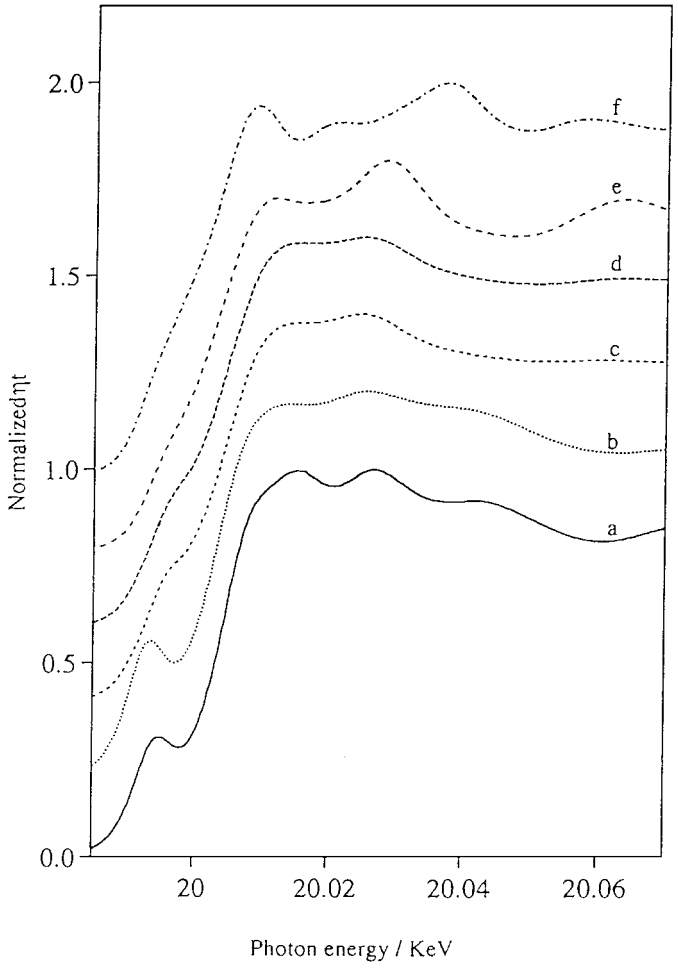

FIG. 6. Mo K edge XANES spectra of (a) MoO_3 crystal; (b) 6 wt% Mo/HZSM-5 (SiO_2/Al_2O_3 ratio of 39.5) after calcined at 873 K for 2 h; (c) after (b) treated with methane at 973 K for 1 h; (d) after (b) treated with methane at 973 K for 24 h; (e) Mo_2C powder; and (f) Mo foil as the reference.

edge features move to lower energy as the oxidation state of Mo is reduced (21), as shown for the Mo/HZSM-5 sample after the reaction with methane at 973 K, compared with those of the calcined sample (Fig. 6b) and MoO_3 (Fig. 6a). The only notable difference between Mo foil and Mo_2C XANES spectra was a separation of the two broad peaks at 20.04 KeV and 20.03 keV above the absorption edge. The XANES spectrum of Mo foil showed a larger separation than the Mo_2C spectrum (Fig. 6e). The XAFS of the Mo/HZSM-5 sample reacted with methane at 973 K for 1 and 24 h (Figs. 6c and 6d) look basically identical to the Mo_2C reference spectrum (Fig. 6e), not to the Mo foil (Fig. 6f).

On the other hand, the corresponding Fourier transform functions are shown in Fig. 7. In Fig. 7, the three dominant peaks on each spectrum represent the Mo-C distance in Mo_2C (1.58 Å), Mo-Mo distance in Mo_2C (2.62 Å), and the Mo-Mo distance in in metallic Mo (2.38 Å) as the reference samples, respectively. These distances should be corrected for phase shifts of 0.34 Å for Mo-Mo and 0.5 Å for Mo-C distances. After the calcination of the 6 wt% Mo loading sample, $(NH_4)_6Mo_7O_{24}$/HZSM-5 at 973 K prior to the methane reaction, the Mo K edge Fourier transform functions showed that the calcined sample (Fig. 7b) consists of the intense peak at 1.42 Å, possibly due to Mo-O bond of highly dispersed Mo oxide species similar to $NaMoO_4$ and $[Mo(=O)_4]$ in NaY as reported by Ozin *et al.* (25). The FT function spectrum (Fig. 7b) is different from that of MoO_3 crystal (Fig. 7a). The EXAFS data suggest that Mo oxide species in the calcined sample of Mo/HZSM-5 is highly dispersed in the internal channels of HZSM-5. The FT function of the sample reacted with the methane at 973 K for 1 h (Fig. 7c) and at 973 K for 24 h (Fig. 7d) showed

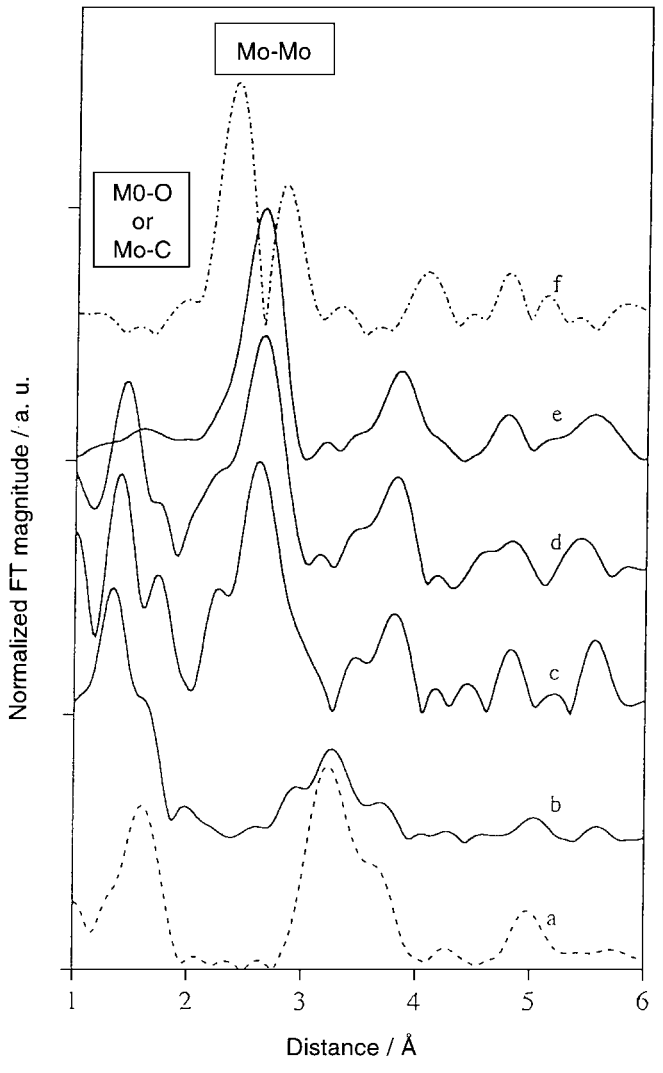

FIG. 7. Mo K edge Fourier transform function spectra of (a) MoO_3 crystal; (b) 6 wt% Mo/HZSM-5 after calcined at 873 K for 2 h; (c) after (b) treated with methane at 973 K for 1 h; (d) after (b) treated with methane at 973 K for 24 h; (e) Mo_2C powder; and (f) Mo foil as the reference.

TABLE 4

EXAFS Parameters for the 3 wt% Mo/HZSM-5 and 6 wt% Mo/HZSM-5 after the Reaction with Methane (1 atm) at 973 K, in Comparison with Those of Mo Foil and Mo_2C

Samples[a]	Mo-Mo			Mo-C(O)		
	C.N.	R (Å)	σ^*	C.N.	R (Å)	σ^{*b}
3 wt% Mo/HZSM-5 973 K—1 h	2.1	2.97	0.084	0.8	2.10	0.047
3 wt% Mo/HZSM-5 973 K—24 h	2.3	2.98	0.087	0.9	2.14	0.055
6 wt% Mo/HZSM-5 973 K—4 h	2.5	2.96	0.095	0.6	2.11	0.028
Mo foil	8	2.72	0.064	—	—	—
Mo_2C powder	12	2.97	0.071	3	2.09	0.047

[a] The samples were stored at 300 K in the EXAFS cell under N_2 atmosphere after the carburization at 973 K.

[b] σ^* = Debye–Waller factor.

peaks at the same positions as those for the Mo_2C reference (Fig. 7e). The spectra of the two samples (Fig. 7c and Fig. 7d) are identical in every detail, except for the peak at 2.23 Å, possibly due to molybdenum oxycarbide. The structural information abstracted from the curve-fitting of the FT function for the samples of Mo/HZSM-5 after the carburization with methane at 973 K are listed in Table 4. The results suggest that the impregnated sample of 3 wt% Mo/HZSM-5 and 6 wt% Mo/HZSM-5 after the calcination at 873 K consists of an isolated Mo oxide, which might be highly dispersed in the internal channels of HZSM-5 (6 Å diameter). After the reaction with methane at 973 K for 1 h and 24 h, the Mo oxide species is converted with methane to Mo_2C cluster (Mo-Mo: C.N. = 2.1–2.5, R = 2.96–2.98 Å; Mo-C: C.N. = 0.8–0.9, R = 2.12–2.14 Å), in comparison with those of the Mo_2C reference (Mo-Mo: C.N. = 12, R = 2.97 Å; Mo-C: C.N. = 3, R = 2.10 Å) (23, 24). The FT function spectra of the Mo/HZSM-5 retained a partial contribution of Mo oxide even after the prolonged carburization with methane at 973 as indicated in Fig. 7. These results imply that the Mo oxide species dispersed in the HZSM-5 framework may migrate at the external surface of the HZSM-5 and be converted with methane to Mo carbide which is highly spread on the support surface and which is active for methane aromatization at 973 K.

The temperature programed reaction (TPR) with methane was conducted on 3 wt% Mo/HZSM-5 using TG/DTA/mass by flowing methane while heating from 300 K to 973 K. As shown in Fig. 8, the evolution of CO (m/e = 28) and H_2 (m/e = 2) occurred at 923–973 K, where the molybdenum oxide is converted to Mo_2C. This initiates the methane conversion to C_2 products (ethene (m/e = 26) + ethane (m/e = 30)), benzene (m/e = 78) and naphthalene (m/e = 128), accompanied with the hydrogen (m/e = 2) evolution. On the other hand, the DTA pattern

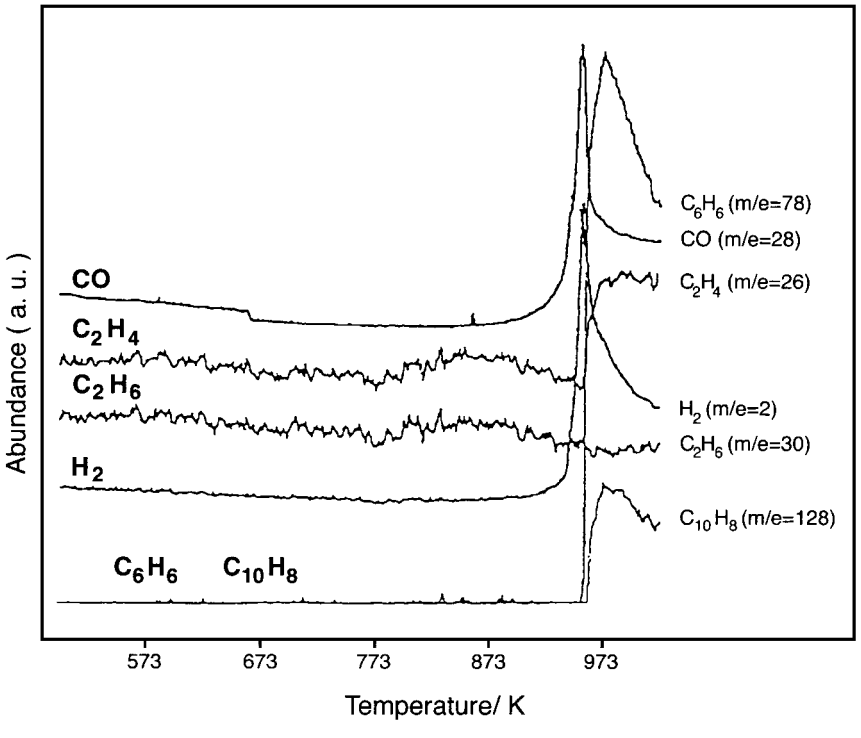

FIG. 8. TPR spectra for the product formation evolved in the reaction with methane on 3 wt% Mo/HZSM-5 (SiO_2/Al_2O_3 ratio of 39.5) by heating from 300 K to 973 K and holding at 973 K for 30 min. Flow rate: CH_4/He = 15/150 (ml/min); ramping rate of temperature: 5 K/min.

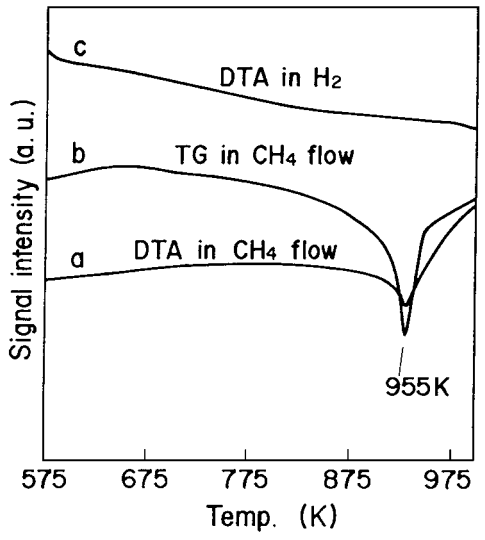

FIG. 9. DTA (a) and TG (b) spectra of 3 wt% Mo/HZSM-5 (SiO_2/Al_2O_3 ratio of 40) in the methane reaction by programmed heating (5 K/min) from 300 K to 973 K and holding at 973 K for 30 min. DTA spectrum (c) of 3 wt% Mo/HZSM-5 (SiO_2/Al_2O_3 ratio of 40) by the programmed heating (5/min) from 300 K to 973 K in a flow of H_2/He (170 ml/min). Flow rate: CH_4/He = 15/150 (ml/min) and H_2/He = 20/150 (ml/min).

(Fig. 9) in the methane stream on the Mo/HZSM-5 shows the distinct endothermic peak at 955 K due to the Mo carbide formation, whereas there is no particular peak in the hydrogen flow (c). The TG pattern in methane flow (a) offers a sharp weight loss at 957 K due to the Mo carbide formation, accompanied by a gradual weight increase above 960 K, possibly owing to the coke formation on the Mo/HZSM-5 in the reaction with methane. These data in XAFS and TG/DTA/mass studies indicate that Mo oxide on HZSM-5 is carburized with methane at 923–963 K to form Mo_2Ç cluster in high dispersion on HZSM-5 which initiates the methane aromatization to benzene and C_2 hydrocarbons at 973 K.

3.6. The Hybrid Catalysts of Molybdenum Carbide and HZSM-5 Supports

From the above discussion it has been known that HZSM-5 as the support is superior to the other materials such as FSM-16 and SiO_2 in methane aromatization reaction, and its Brönsted acididy is an important factor for methane activation and conversion to higher hydrocarbons. But the role of HZSM-5 support and molybdenum species in methane aromatization reaction is still unclear. To discuss on this aspect, two series of hybrid catalysts, 3 wt% Mo/SiO_2 + HZSM-5 ($SiO_2/Al_2O_3 = 40$) and Mo_2C + HZSM-5 ($SiO_2/Al_2O_3 = 40$), were prepared and their catalytic activities were evaluated. In this case, the temperature of the catalyst was elevated to 973 K in helium flow instead of air to prevent the oxidation of Mo_2C. Only trace amounts of higher hydrocarbons such ethene and benzene were produced by flowing methane at 973 K on pure Mo_2C and HZSM-5 (Table 5). The formation rate of benzene in the methane conversion on the physically mixed Mo_2C + HZSM-5 by varying the dilution of Mo_2C, as shown in Fig. 10a. The physically mixed samples were exposed to hydrogen at 723 K for 2 h before testing their effects in the methane conversion. It was demonstrated that a maximum promotion of benzene formation was obtained when Mo_2C was diluted with HZSM-5 in a 5 wt% loading Mo_2C in HZSM-5. Considering the poor mobility of Mo_2C on HZSM-5, the Mo_2C particles (100–500 μm size) are expected to maximize mutual contact of Mo_2C particles at the vicinity of the external surface of HZSM-5. The marked promotion for the benzene yield and methane conversion (Table 5) may be associated with the synergetic effect between Mo_2C and HZSM-5. It is plausible that the CH_x species, due to the dissociative activation of CH_4, may be converted to ethene on the external surface of Mo carbide particle, which migrates and forms benzene and naphthalene at the interface HZSM-5 support having the proper Brönsted acidity.

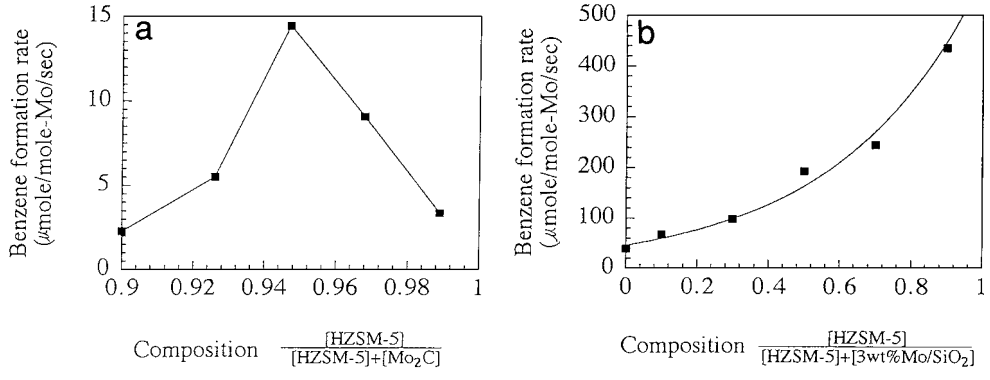

FIG. 10. Variation of the rates of benzene formation (μmol/Mo mol/s) in the methane reaction (SV = 1440 ml/h/g-cat) at 973 K on the hybrid catalysts consisting of [Mo_2C] + [HZSM-5 (SiO_2/Al_2O_3 ratio of 40)] (a) and [Mo/SiO_2] + [HZSM-5 (SiO_2/Al_2O_3 ratio of 40)] (b), depending upon the dilution of Mo components (Mo/SiO_2 and Mo_2C) in the physical mixture systems. Methane 1 atm; flow rate 7.6 ml/min, 973 K. The value of dilution is calculated by the weight of each component in a physical mixture.

TABLE 5

Promotion Effect of Physical Mixing of Mo_2C and 3 wt% Mo/SiO_2 with HZSM-5 (SiO_2/Al_2O_3 Ratio of 39.5) for Benzene Production from Methane at 973 K

Catalyst[b]	CH_4 conversion[a] (%)	Benzene formation rate (μmol/mol-Mo/s)
HZSM-5 ($Si/Al_2 = 39.5$)	0.7	0.42[c]
Mo_2C	0.8	0.3
Mo_2C + HZSM-5 ($Si/Al_2 = 39.5$) (5 wt% Mo loading)	5.7	15
3 wt% Mo/SiO_2	5.3	40
3 wt% Mo/SiO_2 + HZSM-5 ($Si/Al_2 = 39.5$) (1 : 1 volume mixture)	6.2	200
3 wt% Mo/HZSM-5	8.5	316

[a] The reaction condition: methane 1 atm; Flow rate = 7.6 ml/min. The data for methane conversion and product selectivity are taken at the initial stage of the reaction in 40 min after the methane flow passes through the catalyst bed at 973 K.

[b] The physically mixed samples of 0.30 g were amounted in a fixed bed flow-mode pyrex-glass reactor. HZSM-5 (SiO_2/Al_2O_3 ratio of 39.5) and Mo_2C (1.8-μm size, 99% purity, surface area 1–2 m^2/g) were used.

[c] The rate of benzene formation based on μmol/g-HZSM-5/s was taken in the methane conversion under the same reaction condition: 973 K, 1 atm of methane, SV = 1440 ml/h/g-cat.

The combination of 3 wt% Mo/SiO_2 with HZSM-5 ($SiO_2/Al_2O_3 = 40$) also promotes the methane conversion and products such as benzene formation (Table 5), and the benzene formation rate with composition of the 3 wt% Mo/SiO_2 + HZSM-5 ($SiO_2/Al_2O_3 = 40$) is shown in Fig. 10b. The 1 : 1 mixture of 3 wt% Mo/SiO_2 with HZSM-5 shows the highest formation rate of benzene, based on per gram of catalyst, and the benzene formation rate, based on per mole Mo metal, increases monotonously with the decrease of 3 wt% Mo/SiO_2 content (by increasing dilution of the Mo carbide) in the physical mixture. In methane aromatization, a higher methane conversion was obtained on 3 wt% Mo/SiO_2, especially at the early stage of the reaction, but the selectivity towards benzene formation was very low. Most of the converted methane was deposited as surface carbon on the catalyst (above 85% coke selectivity). It is interesting to find that the marked increase in benzene formation on 3 wt% Mo/SiO_2 + HZSM-5, compared to that on 3 wt% Mo/SiO_2, is due to the dilution with HZSM-5 in the physical mixture. The primary products such as CH_x, formed on Mo/SiO_2 are converted to C_2-species such as ethene. C_2-species could diffuse and migrate to the interface of HZSM-5 and be converted into benzene and naphthalene as the aromatic products.

From the above discussion, we suggest the bifunctional catalysis of Mo/HZSM-5 catalysts, consisting of the Mo carbide sites and HZSM-5 having higher Brönsted acidity. Methane is activated on the Mo carbide sites, while HZSM-5 is responsible not only for the further conversion of the primary intermeidates such as CH_x and ethene to higher hydrocarbons and aromatics such as benzene, but also for the reduction of carbon deposition. The two hybrid catalytic systems mentioned above exhibit different catalytic performances for CH_4 aromatization reaction; the formation rate of benzene on 3 wt% Mo/SiO_2 + HZSM-5 with time on-stream has a long induction period before reaching the maximum, similar to that on 3 wt% Mo/HZSM-5, whereas on Mo_2C + HZSM-5 the benzene formation usually decreases at the initial stage and then reaches a steady-state value. These different performances could be explained by the different pathway for the methane activation between Mo_2C and MoO_3. MoO_3 needs to be reduced and carburized with methane to form molybdenum carbide or oxycarbide before it becomes catalytically active for methane aromatization reaction. Compared with Mo_2C + HZSM-5, the higher activity of 3 wt% Mo/SiO_2 + HZSM-5 is related to a higher exposure of Mo/SiO_2 at the interface of the HZSM-5, as has been discussed in Section 3.5.

3.7. Bifunctional Role of Mo_2C and HZSM-5 for the Selective Aromatization of Methane towards Benzene and Naphthalene on Mo/HZSM-5 Catalyst

From the TG/DTA/mass for the temperature-programmed reaction with methane and XAFS studies on the HZSM-5-supported Mo, it is reasonably suggested that the precarburization of Mo oxide on HZSM-5 above 945 K is essential for the formation of highly dispersed Mo carbide (hcp Mo_2C) on HZSM-5, which is remarkably active for the dehydrocyclization of methane to form benzene and naphthalene at the prevailing reaction conditions. As we have disscussed in Sections of 3.4. and 3.6., the HZSM-5 support having optimum Brönsted acidity (SiO_2/Al_2O_3 ratio of 40) provides the Mo carbide-supported catalysts, exhibiting the highest activity and selectivity for the benzene formation and minimizing the coke formation in the methane aromatization. In fact, methane is dehydrogenated on the active Mo carbide (in TG/DTA/mass) to offer the surface carbon species $CH_x (0 < x > 3)$ and H_2 in the gas phase. It is conceivable that the active CH_x and a coupled C_2 species as the primary products which are oligomerized and dehydrocylized to form aromatics such as benzene and naphthalene at the interface of the Brönsted acidic HZSM-5 as presented in Scheme 1. There is a common expectation for the HZSM-5 support to proceed to a further oligomerization reaction of carbon

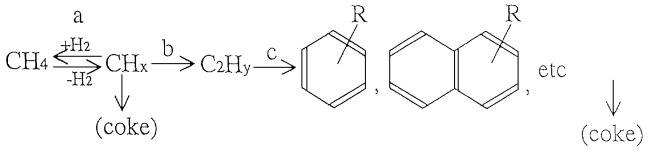

SCHEME 1. (a–b) On an Mo site of carbide or oxycarbide; (c) on HZSM-5.

species to benzene and benzene derivatives by analogy with the catalytic aromatization of methanol and alkanes at 523–623 K, referred to as "Mobil process by HZSM-5" (26). Nevertheless, it is a controversial problem that such an acidic HZSM-5 remains active for the aromatization of alkanes at the extremely high temperatures above 923 K. The evidences of synergitic promotion in the physical mixture of Mo/SiO_2 + HZSM-5 and Mo_2C + HZSM-5 implies that the active carbon species may migrate to HZSM-5 in the vicinity of Mo carbide sites via the formation of C_2 products such as acetylene, ethene, and ethane, which are converted to aromatics such as benzene and naphthalene. In this sense, the bifunctional role of Mo carbide and HZSM-5 for the methane aromatization has a close analogy with the synergetic promotion on Pt/alumina catalysts for the alkane reforming process, consisting of the dehydrogenation of alkanes to olefins catalyzed on Pt sites which migrate to the acidic alumina support, resulting in the dehydrocyclization to benzene derivatives. In addition, Boudart *et al.* (24) have reported previously that Mo carbide is catalytically active for the dehydrogenation towards olefins and hydrogenolysis of alkanes, similar to the typical noble metals such as Pt and Ir.

4. CONCLUSION

The present work may be summerized by the following conclusions;

(1) Among the supports such as FSM-16, Mordenite, USY, alumina, and SiO_2, 3 wt% Mo-loading catalysts using HZSM-5 offer the highest activities and selectivities for aromatic products such as benzene and naphthalene in the methane conversion at 973 K and 1 atm.

(2) The TG/DTA/mass and EXAFS studied reveal that the Mo oxide supported on HZSM-5 is endothermically converted at 955 K with methane in evolving H_2 and CO to molybdenum carbide Mo_2C, which initiates the methane conversion around 960 K, yielding benzene, naphthalene, and C_2 hydrocarbons such as ethene as hydrocarbon products.

(3) The IR measurements in pyridine adsorption reveal that Mo/HZSM-5 catalysts having the optimum SiO_2/Al_2O_3 ratio between 20 and 70 show the maximum Brönstead acidity among the catalysts with the SiO_2/Al_2O_3 ratio of 20–1900. There is a close correlation between the benzene formation in the methane conversion and their Brönsted acidity, regardless of the Lewis acidity of the Mo/HZSM-5 catalysts. The highest benzene formation and minimizing of coke formation are obtained on the Mo/HZSM-5 having the SiO_2/Al_2O_3 ratio of 40.

(4) A remarkable synergetic promotion in benzene formation exists for the hybrid catalysts consisting of 3 wt% Mo/SiO_2 + HZSM-5 and Mo_2C + HZSM-5, whereas each component by itself shows marginal activity in the reaction.

(5) This bifunctional catalysis of Mo_2C/HZSM-5 for a methane aromatization reaction is discussed by analogy with the synergetic promotion on Pt/Al_2O_3 catalyst for the dehydroaromatization of alkanes.

ACKNOWLEDGMENTS

This work was supported by the Proposal-Based New Industry Creative Type Technology R&D Promotion Program from the New Energy and Industrial Technology Development Organization (NEDO) of Japan. The authors thank Dr. Inagaki and Dr. Fukushima, Toyota Central Research Laboratory, for their gifts of the mesoporous materials of FSM-16, and helpful discussion on the bifunctional role of the supports for the methane dehydroaromatization on the Mo catalysts.

REFERENCES

1. Fox III, J. M., *Catal. Rev.-Sci. Eng.* **35**(2), 169 (1993).
2. Brown, M. J., and Parkyns, N. D., *Catal. Today* **8**, 305 (1991).
3. Kuo, J. C. W., Kresge, C. T., and Palermo, R. E., *Catal. Today* **4**, 463 (1989).
4. Krylov, O. V., *Catal. Today* **18**, 209 (1993).
5. Guczi, L., van Santen, R. A., and Sayma, K. V., *Catal. Rev.-Sci. Eng.* **38**, 249 (1996).
6. Lunsford, J., *Catal. Today* **6**, 235 (1990).
7. Wang, L., Tao, L., Xie, M., Xu, G., Huang, J., and Xu, Y., *Catal. Lett.* **21**, 35 (1993).
8. Xu, Y., Liu, S., Wang, L., Xie, M., and Guo, X., *Catal. Lett.* **30**, 135 (1995).
9. Solymosi, F., Erdöhelyi, A., and Szöke, A., *Catal. Lett.* **32**, 43 (1995).
10. Solymosi, F., Szöke, A., and Cserényi, J., *Catal. Lett.* **39**, 157 (1996).
11. Szöke, A., and Solymosi, F., *Appl. Catal. A: General* **142**, 361 (1996).
12. Solymosi, F., Cserényi, J., Szöke, A., Bánsagi, T., and Oszkó, A., *J. Catal.* **165**, 156 (1997).
13. Wang, S.-T., Xu, Y., Wang, L., Liu, S., Li, G., Xie, M., and Guo, X., *Catal. Lett.* **38**, 39 (1996).
14. Xu, Y., Shu, Y., Liu, S., Huang, J., and Guo, X., *Catal. Lett.* **35**, 233 (1995).
15. Liu, W., Xu, Y., Wong, S.-T., Qiu, J., and Yang, N., *J. Mol. Catal. A: Chemical* **120**, 257 (1997).
16. Wang, D., Lunsford, J. H., and Rosynek, M. P., *J. Catal.* **169**, 347 (1997).
17. Wang, D., Rosynek, M. P., and Lunsford, J. H., *Topics Catal.* **3**, 289 (1996).
18. Liu, S., Dong, Q., Ohnishi, R., and Ichikawa, M., *J.C.S. Chem. Commun.*, 1455 (1997).
19. Liu, S., Dong, Q., Ohonishi, R., and Ichikawa, M., *Chem. Commun.*, 1217 (1998).
20. User Manual of Technos EXAFS analyzing Program.
21a. Basila, M. R., Kanter, T. R., and Rhee, K. H., *Nature* **68**, 3197 (1964).
21b. Poncelet, G., and Dubru, M. L., *J. Catal.* **52**, 321 (1978).
22. Mirodetos, C., and Barthomeuf, D., *J. Catal.* **57**, 136 (1979).
23. Lee, J. S., and Boudart, M., *Catal. Lett.* **20**, 97 (1993).
24. Lee, J. S., Locatelli, S., Oyama, S. T., and Boudart, M., *J. Catal.* **125**, 157 (1990).
25. Ozin, G. A., Prokorowitcz, P. A., and Ozkar, S., *J. Am. Chem. Soc.* **114**, 8957 (1992).
26a. Olson, D. H., Lago, R. M., and Haag, W. O., *J. Catal.* **61**, 390 (1980).
26b. Lago, R. M., Haag, W. O., Mikovsky, R. J., Olson, D. H., Hellring, S. D., Scmitt, K. D., and Kerr, G. T., *Stud. Surf. Sci. Catal.* **28**, 661 (1986).